Vibrational Structure in the Photoelectron Spectrum of Cyclobutadiene as a Probe of Structure

Daniel W. Kohn and Peter Chen*[1]

Contribution from the Mallinckrodt Chemical Laboratory, Harvard University, Cambridge, Massachusetts 02138

Received May 26, 1992. Revised Manuscript Received October 6, 1992

Abstract: The photoelectron spectrum of cyclobutadiene, c-C_4H_4, is reported with partial resolution of vibrational structure. Model calculations of the Franck–Condon envelope in the spectrum, based on ab initio geometries and force constants for c-C_4H_4 and c-$C_4H_4^{\bullet+}$, find a surprisingly good agreement for a transition from the rectangular neutral to a rectangular, as opposed to a rhomboidal or square, radical cation. An adiabatic ionization potential of 8.16 ± 0.03 eV is also determined. The spectrum confirms that correlation between σ and π electrons is needed in ab initio calculations for $C_4H_4^{\bullet+}$ to obtain even a qualitatively correct geometry for the Jahn–Teller-distorted ion.

Introduction

We report the photoelectron spectrum of cyclobutadiene (**1**), c-C_4H_4, produced by the flash pyrolysis of tricyclo[2.1.0.0^{2,5}]pentan-3-one (**2**) in a supersonic jet expansion. While there has been one previous report[2] of the photoelectron spectrum of **1**, the spectrum reported in this work shows better vibrational resolution, which we attribute to jet-cooling in the supersonic expansion and a different electron energy analyzer. Previous applications of photoelectron spectroscopy to polyatomic organic molecules have usually sought ionization potentials[3] or orbital splittings[4] and, accordingly, made little use of any vibrational structure that may have appeared. We explicitly employ vibrational structure in the spectrum as a probe of the potential surfaces of **1** and $\mathbf{1}^{\bullet+}$ via comparisons of the observed photoelectron spectrum to calculated Franck–Condon factors. We find that the equilibrium geometry of $\mathbf{1}^{\bullet+}$, the radical cation of cyclobutadiene, is rectangular, as in cyclobutadiene itself,[5] although the deviation from a square is less than in **1**. Comparisons to the simulations for square and rhomboidal geometries rule out those structures.

1 and $\mathbf{1}^{\bullet+}$ are prototypes for pseudo-Jahn–Teller-[6] and Jahn–Teller-distorted[6] molecules, respectively. From simple molecular orbital considerations for a structure set to a D_{4h} geometry, one finds that **1** has two electrons in the degenerate e_g HOMO. Using symmetry considerations, this electronic configuration leads to the terms in the symmetric product $e_g \otimes e_g = a_{1g} \oplus b_{1g} \oplus b_{2g}$. Of these, ab initio calculations for the square geometry[7] find the lowest singlet and triplet states of **1** to be $^1B_{1g}$ and $^3A_{1g}$. With only a single electron in the degenerate e_g orbital, the ground state of the cyclobutadiene radical cation,[8] $\mathbf{1}^{\bullet+}$, is ^2E_g at a D_{4h} geometry. The Jahn–Teller theorem[6] indicates that $\mathbf{1}^{\bullet+}$, being electronically degenerate at its most symmetric geometry, must necessarily distort along a non-totally-symmetric coordinate to a minimum that has lower symmetry. For **1**, which is not electronically degenerate despite its orbital degeneracy, there is no *first-order* Jahn–Teller distortion, but rather a second-order, or pseudo-Jahn–Teller, effect. Accordingly, both **1** and $\mathbf{1}^{\bullet+}$ have been predicted to distort from a square geometry, with **1** going to a rectangle and $\mathbf{1}^{\bullet+}$ going to either a rectangle or a rhombus. Experimental verification[5] of a D_{2h} equilibrium geometry for cyclobutadiene comes from the number of IR absorption bands in matrix-isolated **1** (and isotopomers) and chemical trapping[9] of isotopically-labeled **1**. No experiment pertaining to the structure of the radical cation has thus far appeared. We undertake a study of the C_4H_4 system by photoelectron spectroscopy to address these problems of structure. More generally, the interactions within the cyclobutadiene system, investigated here, pertain to the generic organic biradical in that the degenerate HOMO occupied by two electrons (for a biradical), or one electron (for the analogous radical cation), should induce large vibronic interactions of the type seen in the C_4H_4 system, with concomitant geometric distortion.

Scheme I

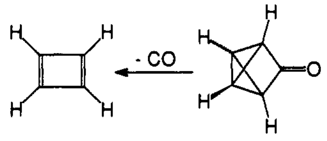

1 2

In this report, we implement the simulation of the Franck–Condon envelope observed in our photoelectron spectrum of **1** within a harmonic approximation,[10,11] which, at first sight, seems inappropriate for the problem at hand. However, we justify the model by consideration of the form of the potential surfaces that

---

[1] National Science Foundation Presidential Young Investigator, David and Lucile Packard Fellow, Camille and Henry Dreyfus Teacher-Scholar, and Alfred P. Sloan Research Fellow.

[2] Kreile, J.; Münzel, N.; Schweig, A.; Specht, H. *Chem. Phys. Lett.* **1986**, *124*, 140.

[3] For recent reviews, see: Westwood, N. P. C. *Chem. Soc. Rev.* **1989**, *18*, 317. Blush, J. A.; Clauberg, H.; Kohn, D. W.; Minsek, D. W.; Zhang, X.; Chen, P. *Acc. Chem. Res.* **1992**, *25*, 385.

[4] For a representative example, see: Gleiter, R.; Kratz, G.; Schäfer, W.; Schehlmann, V. *J. Am. Chem. Soc.* **1991**, *113*, 9258. A compilation and a review are given by: Kimura, K.; Katsumata, S.; Achiba, Y.; Yamazaki, T.; Iwata, S. *Handbook of HeI Photoelectron Spectra of Fundamental Organic Molecules*; Halsted Press: New York, 1981.

[5] Good reviews of the extensive literature: Bally, T.; Masamune, S. *Tetrahedron* **1980**, *36*, 343. Maier, G. *Angew. Chem., Int. Ed. Engl.* **1988**, *27*, 309. Arnold, B.; Michl, J. In *Kinetics and Spectroscopy of Carbenes and Biradicals*; Platz, M. S., Ed.; Plenum: New York, 1990; Chapter 1.

[6] For reviews, see: Sturge, M. D. *Solid State Phys.* **1967**, *20*, 91. Englman, R. *The Jahn–Teller Effect in Molecules and Crystals*; Wiley: New York, 1972. Fischer, G. *Vibronic Coupling*; Academic Press: New York, 1984.

[7] Jafri, J. A.; Newton, M. D. *J. Am. Chem. Soc.* **1978**, *100*, 5012. Borden, W. T.; Davidson, E. R.; Hart, P. *J. Am. Chem. Soc.* **1978**, *100*, 388.

[8] Borden, W. T.; Davidson, E. R.; Feller, D. *J. Am. Chem. Soc.* **1981**, *103*, 5725.

[9] Whitman, D. W.; Carpenter, B. K. *J. Am. Chem. Soc.* **1982**, *104*, 6473.

[10] For an application of Franck–Condon simulations to determination of the structure of $C_3H_2^{\bullet+}$, see: Clauberg, H.; Chen, P. *J. Phys. Chem.* **1992**, *96*, 5676.

[11] Calculation of Franck–Condon factors for polyatomic molecules in mass-weighted Cartesian coordinates are described by: Kohn, D. W.; Robles, E. S. J.; Logan, C. F.; Chen, P. *J. Phys. Chem.*, submitted for publication. Warshel, A.; Karplus, M. *Chem. Phys. Lett.* **1972**, *17*, 7. Warshel, A.; Karplus, M. *J. Am. Chem. Soc.* **1974**, *96*, 5677. Warshel, A. *J. Chem. Phys.* **1975**, *62*, 214. Özkan, I. *J. Mol. Spectrosc.* **1990**, *139*, 147.

0002-7863/93/1515-2844$04.00/0

result from the vibronic Hamiltonian for $1^{\bullet+}$. A full anharmonic treatment in which the vibronic wave functions for the multidimensional double-well potential are expressed as expansions in a suitable basis is underway. Nevertheless, the present harmonic treatment highlights certain physically relevant features of the potential which result from the magnitudes of the Jahn–Teller stabilization energies and are therefore of importance in and of themselves.

Experimental Section

The supersonic jet flash pyrolysis technique for generating high-number densities of reactive intermediates with the molecular beam time-of-flight mass and photoelectron spectrometers has been previously described.[12] Several potential thermal precursors[13] were prepared and pyrolyzed to check for clean, specific conversion to **1**. The best precursor was found to be tricyclo[2.1.0.0^{2,5}]pentan-3-one (**2**), which we prepared according to a procedure of Maier et al.,[14] with some modifications. In particular, the carbenoid addition steps are improved, and the desilylation is done prior to final cyclization to improve the overall yield.

Ethyl 2,3-Bis(trimethylsilyl)-2-cyclopropene-1-carboxylate (3). **3** is prepared by adding a solution of ethyl diazoacetate (60 mL, 570 mmol), diluted with 660 mL of bis(trimethylsilyl)acetylene, from a syringe pump over $3^1/_2$ days to a well-stirred solution of rhodium(II) octanoate dimer (2.0 g, 2.5 mmol) in 400 mL of bis(trimethylsilyl)acetylene. For the first $^1/_2$ h of the addition, the Rh(II) solution is maintained at 60 °C. Thereafter, the addition is done at room temperature. Bis(trimethylsilyl)acetylene is distilled (25 Torr, 48 °C) through a large Vigreaux column, and the residue fractionally distilled (0.25 Torr, 79 °C), to yield **3** as a slightly yellow clear oil (46.5 g, 181 mmol, 34.4%). [^{1}H NMR (CDCl$_3$): δ 4.04 (q, 2 H), 1.86 (s, 1 H), 1.18 (t, 3 H), 0.18 (s, 18 H).]

2,3-Bis(trimethylsilyl)-2-cyclopropene-1-carboxylic Acid (4). The carboxylic acid, **4**, is prepared by a non-nucleophilic hydrolysis of the ethyl ester. Note that the formation of the intermediate silyl ester requires rigorously anhydrous conditions, most importantly, the vacuum drying (180 °C, 10 h) of the NaI. The ester, **3** (237 mmol, 60.8 g), chlorotrimethylsilane (33.1 mL, 260 mmol), NaI (39.1 g, 260 mmol), and acetonitrile (259 mL) are stirred at reflux for 20 h. The solution is cooled to room temperature, the reaction is quenched with 250 mL of water, and the mixture is stirred for 1 h. The solution is distilled at atmospheric pressure until the distillate temperature reaches 100 °C. The solution is then saturated with NaCl. As the solution cools to room temperature, most of the acid crystallizes and is separated from the aqueous solution. The remaining acid is extracted with diethyl ether (10 × 40 mL), and the extract is dried over MgSO$_4$ and rotovaped to yield the crude acid (49.35 g, 216 mmol, 91.1%). [^{1}H NMR (CDCl$_3$): δ 1.82 (s, 1 H), 0.19 (s, 18 H).] The crude product may be recrystallized from *n*-pentane to yield white crystals (mp 89.7–90.7 °C); however, it is best to proceed with the crude acid and purify during the next step, at the acid bromide, to get the highest overall yield.

2-Diazo-1-[2,3-bis(trimethylsilyl)-2-cyclopropen-1-yl]ethanone (5). The diazo ketone, **5**, is prepared by reaction of diazomethane with the corresponding acid bromide. To 49.4 g (216 mmol) of **4** and 125 mL of CH$_2$Cl$_2$ is added a 2 M solution of oxalyl bromide (270 mmol, 135 mL) at 25 °C over 1 h. The solvent is removed at aspirator pressure and room temperature, and the residue distilled (0.25 Torr, 58 °C), yielding 59.2 g (203 mmol, 94.1%) of the acid bromide as a red oil. [^{1}H NMR (CDCl$_3$): δ 2.32 (s, 1 H), 0.25 (s, 18 H).] A –30 °C solution of distilled diazomethane (406 mmol) and diethyl ether (1020 mL) is added over 2 h to a –78 °C solution of the acid bromide (203 mmol) in diethyl ether (300 mL). The solution is stirred for an additional 1 h at –78 °C and then transferred to a –30 °C bath for 20 h. The solution is then purged for 1 h with N$_2$ as it is allowed to warm to room temperature. The yield is 0.158 M × 1.27 L = 201 mmol of crude product (99%). [^{1}H NMR (CDCl$_3$): δ 4.76 (s, 1 H), 2.05 (s, 1 H), 0.20 (s, 18 H).]

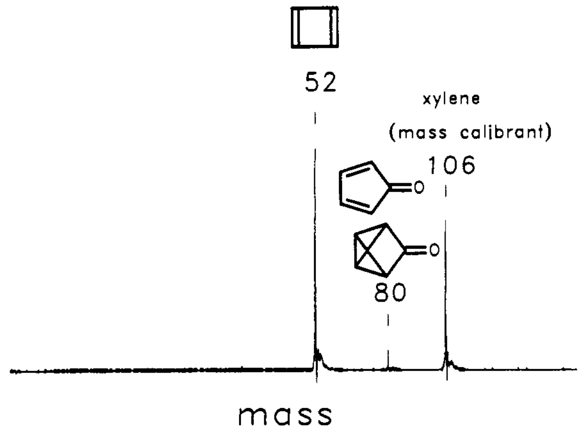

Figure 1. 10.49-eV photoionization mass spectrum of pyrolyzed tricyclo[2.1.0.0^{2,5}]pentan-3-one (**2**). Only *m/e* = 52 (cyclobutadiene) and *m/e* = 80 (cyclopentadienone) appear. Note the absence of any dimers, *m/e* = 104, or dimer-derived products, e.g. C$_6$H$_6$ at *m/e* = 78.

Tricyclo[2.1.0.0^{2,5}]pentan-3-one (2). The diazo ketone, **5**, is desilylated to give 2-diazo-1-(2-cyclopropen-1-yl)ethanone by treatment of 1.13 L (179 mmol) of the ethereal solution with aqueous methanolic K$_2$CO$_3$ (260 g in 750 mL of H$_2$O and 375 mL of MeOH) and stirring the mixture for 15 min at room temperature. The ether phase is then separated from the mixture and combined with a single ethereal extraction (100 mL) of the aqueous phase. After drying over CaCl$_2$ and evaporation of the ether, the deprotected diazo ketone is taken up in a solution of 500 mL of CHCl$_3$ and 1 mL of triethylamine. [^{1}H NMR (CDCl$_3$): δ 6.92 (s, 2 H), 5.15 (s, 1 H), 2.25 (br s, 1 H).] Because of the facile dimerization of the deprotected diazo ketone, the final carbenoid addition is performed without any delay or purification. The CHCl$_3$ solution of the diazo ketone is added dropwise over 45 min to a refluxing solution of rhodium(II) octanoate dimer (1.4 g, 1.8 mmol) in CHCl$_3$ (720 mL). The solution is refluxed for an additional 45 min, cooled, and distilled through a Vigreaux column. The CHCl$_3$ is distilled off at atmospheric pressure (<61 °C), first through the large Vigreaux column and then through a short-path vacuum-jacketed still. The volatile residue is then trap-to-trap separated (0.25 Torr, 25 °C) into a –196 °C cooled collector. Residual CHCl$_3$ is then removed at reduced pressure, leaving an oil comprising 30% **2**, as judged by NMR integrations. Chromatography with CHCl$_3$ (1% triethylamine) on silica gel (100–200 mesh) yields 400 mg (5.0 mmol) of pure **2**; overall yield is 2.5% from **5**. The product, **2**, can be stored for months as a neat liquid at –5 °C, with no change in the mass or NMR spectrum. [^{1}H NMR (CDCl$_3$): δ 3.99 (t, 2 H), 2.06 (t, 2 H).]

Results

Ionization with 118.2-nm photons (10.49 eV) gave a mass spectrum of unpyrolyzed **2** showing a single peak at *m/e* = 52, presumably from rapid decarbonylation of the parent molecular ion (*m/e* = 80) of structure $2^{\bullet+}$. Flash pyrolysis (1200 K/10 μs) of **2**, seeded ≈1% in 1300 Torr of helium, gave a mass spectrum with a large *m/e* = 52 peak and a small *m/e* = 80 peak, shown in Figure 1. Photoelectron spectra taken with and without pyrolysis are very different. The pyrolysate was found to be cyclobutadiene[2] (major product), cyclopentadienone[15] (minor product), and residual **2**. In particular, the mass and photoelectron spectra show the complete absence of any C$_8$H$_8$ species, or the C$_6$H$_6$ resulting from cracking of cyclobutadiene dimers. Application of a small retarding potential to the photoelectrons improved our energy resolution and excluded all electrons not due to **1**. The resulting photoelectron spectrum is shown in Figure 2. The adiabatic ionization potential of cyclobutadiene, read directly from the spectrum, is 8.16 ± 0.03 eV, in good agreement with Kreile[2] et al.

Discussion

Cyclobutadiene has been the subject of numerous experimental and computational studies,[5] with recent interest piqued by the

---

(12) Blush, J. A.; Park, J.; Chen, P. *J. Am. Chem. Soc.* **1989**, *111*, 8951. Minsek, D. W.; Chen, P. *J. Phys. Chem.* **1990**, *94*, 8399. Clauberg, H.; Chen, P. *J. Am. Chem. Soc.* **1991**, *113*, 1445. Clauberg, H.; Minsek, D. W.; Chen, P. *J. Am. Chem. Soc.* **1992**, *114*, 99. Minsek, D. W.; Blush, J. A.; Chen, P. *J. Phys. Chem.* **1992**, *96*, 2025. Zhang, X.; Chen, P. *J. Am. Chem. Soc.* **1992**, *114*, 3147. Blush, J. A.; Chen, P. *J. Phys. Chem.* **1992**, *96*, 4138. Kohn, D. W.; Clauberg, H.; Chen, P. *Rev. Sci. Instrum.* **1992**, *63*, 4003.

(13) Maier, G.; Hoppe, M.; Lanz, K.; Reisenauer, H. P. *Tetrahedron Lett.* **1984**, *25*, 5645.

(14) Maier, G.; Hoppe, M.; Reisenauer, H. P. *Angew. Chem., Int. Ed. Engl.* **1983**, *22*, 990. Hoppe, M. Inaugural Dissertation, University of Giessen, Germany, 1984.

(15) For a spectrum of cyclopentadienone for comparison, see: Eck, V.; Lauer, G.; Schweig, A.; Thiel, W.; Vermeer, H. *Z. Naturforsch. A* **1978**, *33A*, 383.

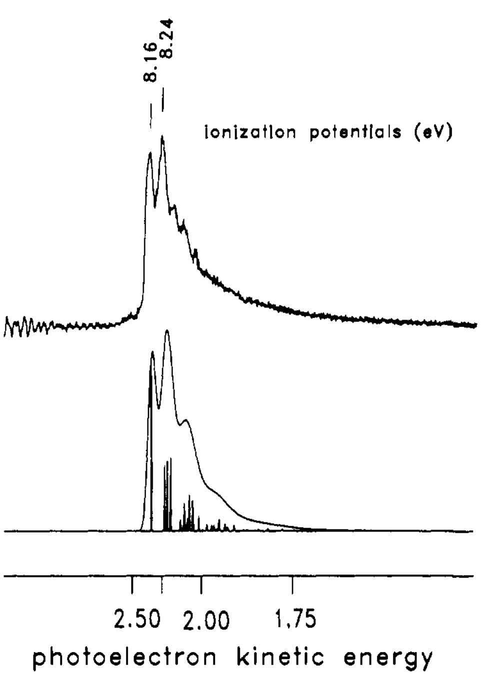

Figure 2. 10.49-eV time-of-flight photoelectron spectrum of cyclobutadiene and a simulation of rectangular **1** going to rectangular $\mathbf{1}^{\cdot+}$. Ionization potentials and photoelectron kinetic energies are in electronvolts and are determined to ±0.03 eV in absolute calibration. Three of the four a_g normal modes (in D_{2h} notation) are found to give significant intensity: ν_1 (symmetric HCC in-plane bend), ν_2 (symmetric C—C stretch), and ν_3 (symmetric C═C stretch). The fourth a_g mode, ν_4 (symmetric C—H stretch), shows no significant activity. The 6-31G+*/MP2 frequencies are scaled to match the known infrared spectrum of cyclobutadiene. The geometries for **1** and $\mathbf{1}^{\cdot+}$ are listed in Table I.

suggestion that automerization proceeds predominantly by heavy-atom tunneling *through* the barrier separating two identical minima.[16] We have been exploring[10] the calculation of polyatomic Franck–Condon factors for molecules in which ionization is accompanied by a change in equilibrium geometry (Duschinsky rotation[17,18]). Because Franck–Condon factors depend sensitively[11] on differences between the potential surfaces of the neutral and the cation, a photoelectron spectrum ought to depend on the extent of distortion from a D_{4h} geometry for pseudo-Jahn–Teller-distorted **1** and Jahn–Teller-distorted $\mathbf{1}^{\cdot+}$. We give the results for the simplest physically reasonable simulation of the vibrational structure in the photoelectron spectrum of **1** using harmonic potentials centered on the D_{2h} ab initio equilibrium geometries of **1** and $\mathbf{1}^{\cdot+}$. Because we have shown that our supersonic jet expansion cools vibrations efficiently,[12] all of the bands in the photoelectron spectrum of **1** originate in the vibronic ground state of **1**, well below the top of the barrier for automerization. Because only the vibronic ground state of **1** is involved in observed transitions, modeling the vibrational wave function of **1** using unperturbed harmonic oscillators is reasonable. A quick check with a one-dimensional double-well potential (Gaussian-perturbed oscillator[19]) found that, for a barrier height of ≈10 kcal/mol, the $\nu = 0$ wave function is essentially that of an unperturbed harmonic oscillator centered at the bottom of the local well. Use of harmonic oscillator wave functions for $\mathbf{1}^{\cdot+}$ is much harder to justify because bands were observed going to levels well up into the regions where vibronic interactions cannot be ignored. We will make that justification, though, in the course of discussing the Jahn–Teller stabilization energies for $\mathbf{1}^{\cdot+}$ and their effects on vibronic energy levels and wave functions. These assumptions allow us to do sufficiently realistic Franck–Condon simulations to distinguish between square, rectangular, and rhomboidal geometries for $\mathbf{1}^{\cdot+}$.

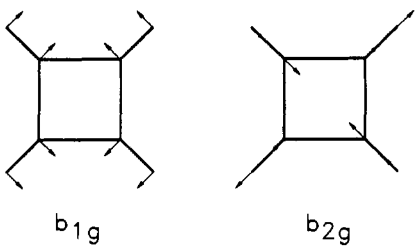

Figure 3. Normal modes in D_{4h} that should give large first-order Jahn–Teller stabilization energies for $\mathbf{1}^{\cdot+}$.

A Model for Vibronic Coupling in $\mathbf{1}^{\cdot+}$. We start with a simplified model of the vibronic interactions that cause the Jahn–Teller effect in $\mathbf{1}^{\cdot+}$. Only for those cases where the most symmetric geometry of a molecule belongs to one of the tetragonal point groups, i.e. C_4, C_{4v}, C_{4h}, D_4, D_{4h}, or S_4, are the Jahn–Teller-active modes nondegenerate.[20–22] For $\mathbf{1}^{\cdot+}$, distortions along b_{1g} and b_{2g} vibrational coordinates should give a first-order energy lowering. If we make the reasonable assumption that the particular b_{1g} and b_{2g} vibrations for which there are large Jahn–Teller interactions are those which involve CC skeletal motions, then we find two active vibrational modes at the square geometry, depicted in Figure 3, that correspond to rectangular and rhomboidal distortions. The Jahn–Teller effect for $\mathbf{1}^{\cdot+}$ is therefore a $E_g \otimes b_{1g} \otimes b_{2g}$ problem and represents one of the simplest multimode coupling problems that can be constructed.

Ignoring spin–orbit coupling, the simplest vibronic Hamiltonian for a two-state, two-mode ($E_g \otimes b_{1g} \otimes b_{2g}$) problem can be written[6]

$$\boldsymbol{H} = \frac{1}{2}\left(\frac{P_1^2}{\mu_1} + \mu_1\omega_1^2 Q_1^2\right) + \frac{1}{2}\left(\frac{P_1^2}{\mu_1} + \mu_1\omega_1^2 Q_1^2\right) + \begin{bmatrix} -V_1Q_1 & V_2Q_2 \\ V_2Q_2 & V_1Q_1 \end{bmatrix} \tag{1}$$

where Q_1 and Q_2 are the b_{1g} and b_{2g} normal coordinates (defined at the square geometry), with P_i, V_i, μ_i and ω_i being the corresponding conjugate momenta, Jahn–Teller coupling coefficients, reduced masses, and angular frequencies for the two modes. The first two terms are just the Hamiltonian for the two unperturbed harmonic oscillators at a square geometry. The third term includes all of the vibronic interactions. Diagonalization of the Hamiltonian in a suitable basis,[20] e.g. product functions of the two components of the degenerate electronic state with the unperturbed harmonic oscillator wave functions, would give explicit vibronic energies and wave functions as expansions in that basis. Some qualitative generalizations may be made, though, without resort to a general solution of the vibronic coupling problem.

With only linear coupling[23] in the third term of the vibronic Hamiltonian, there can be a minimum at a rectangular geometry for $\mathbf{1}^{\cdot+}$ or a rhomboidal geometry, *but not both*. There have been no experimental data to distinguish between the two possibilities. If $V_1 > V_2$, then rectangular $\mathbf{1}^{\cdot+}$ is a minimum in energy, while rhomboidal $\mathbf{1}^{\cdot+}$ is a saddle point connecting the two rectangular

---

[16] Carpenter, B. K. *J. Am. Chem. Soc.* **1983**, *105*, 1700. Huang, M. J.; Wolfsberg, M. *J. Am. Chem. Soc.* **1984**, *106*, 4039. Dewar, M. J. S.; Merz, K. M.; Stewart, J. J. P. *J. Am. Chem. Soc.* **1984**, *106*, 4040. Carsky, P.; Bartlett, R. J.; Fitzgerald, G.; Noga, J.; Spirko, V. *J. Chem. Phys.* **1988**, *89*, 3008. Carsky, P.; Spirko, V.; Hess, B. A.; Schaad, L. J. *J. Chem. Phys.* **1990**, *92*, 6069. Orendt, A. M.; Arnold, B. R.; Radziszewski, J. G.; Facelli, J. C.; Malsch, K. D.; Strub, H.; Grant, D. M.; Michl, J. *J. Am. Chem. Soc.* **1988**, *110*, 2648. Arnold, B. R.; Radziszewski, J. G.; Campion, A.; Perry, S. S.; Michl, J. *J. Am. Chem. Soc.* **1991**, *113*, 692.

[17] Duschinsky, F. *Acta Physicochim. URSS* **1937**, *7*, 551.

[18] Sharp, T. E.; Rosenstock, H. M. *J. Chem. Phys.* **1964**, *41*, 3453. Botter, R.; Dibeler, V. H.; Walker, J. A.; Rosenstock, H. M. *J. Chem. Phys.* **1966**, *44*, 1271. Rosenstock, H. M. *Int. J. Mass Spectrom. Ion Phys.* **1971**, *7*, 33.

[19] Chan, S. I.; Stelman, D. *J. Chem. Phys.* **1963**, *39*, 545.

[20] Child, M. S. *Mol. Phys.* **1960**, *3*, 601. Muramatsu, S.; Sakamoto, N. *J. Phys. Soc. Jpn.* **1978**, *44*, 1640. Hoffman, B. M.; Ratner, M. A. *Mol. Phys.* **1978**, *35*, 901.

[21] Hougen, J. T. *J. Mol. Spectrosc.* **1964**, *13*, 149.

[22] Ballhausen, C. J. *Theor. Chim. Acta* **1965**, *3*, 368.

[23] Quadratic coupling causes some additional complications but is ignored in the present treatment. See: Bacci, M. *Phys. Rev. B* **1978**, *17*, 4495.

Table I. Optimum Rectangular Structure for **1**, Rectangular $\mathbf{1}^{\cdot+}$, Rhomboidal $\mathbf{1}^{\cdot+}$, and Square $\mathbf{1}^{\cdot+}$ at the 6-31G+*/MP2 Level

	rectangular c-C_4H_4 ab initio	rectangular c-$C_4H_4^{\cdot+}$ ab initio	rectangular c-$C_4H_4^{\cdot+}$ best fit	square c-$C_4H_4^{\cdot+}$ ab initio	rhomboidal c-$C_4H_4^{\cdot+}$ ab initio
$r_{C=C}$ (Å)	1.3470	1.3854	1.3854	1.4350	1.4344
r_{C-C}	1.5648	1.4974	1.4854		
r_{C-H} (Å)	1.0843	1.0853	1.0853	1.0847	1.0894, 1.0806
∠HCC (deg)	134.75	135.0	135.0	135.0	133.50, 136.50
∠CCC (deg)	90.0	90.0	90.0	90.0	93.01, 86.99
E (hartrees)	−154.175 799 4	−153.899 088 5		−153.884 044	−153.886 317
ΔE (eV)	0	7.529		7.939	7.877

minima. If $V_2 > V_1$, the minima and saddle points are reversed. In either case, the square structure is a cusp on the potential surface. In the only previous calculation on $\mathbf{1}^{\cdot+}$, Borden[8] found that the relative ordering of the rectangular and rhomboidal structures of $\mathbf{1}^{\cdot+}$ showed a marked dependence on the level of the calculation. The rhomboidal structure was found to be lower at the RHF level and lower yet at the UHF level. Addition of CI among π-excitation decreased the difference but left the rhombus lower in energy than the rectangle. Only when CI among π- and σ-excitations was included did the energy of rectangular $\mathbf{1}^{\cdot+}$ fall below that of rhomboidal $\mathbf{1}^{\cdot+}$. At the optimum rectangular and rhomboidal geometries, the Jahn–Teller stabilization energies, relative to the square, were reported to be 7.0 and 1.0 kcal/mol, respectively.

Justification for a Harmonic Model Potential for $\mathbf{1}^{\cdot+}$. While the application of a general solution for the Hamiltonian in eq 1 will be the subject of a separate report, a limiting case can be examined which suggests that a simple harmonic model will be close to the more complete solution *for this particular case*. As has been noted by Ballhausen[22] and by Hougen,[21] the case where $V_2 \ll V_1$, or effectively $V_2 = 0$, admits to an interesting solution. Following the treatment by Ballhausen,[22] we rewrite eq 1 to get

$$H=\frac{1}{2}\left(\frac{P_1^2}{\mu_1}+\mu_1\omega_1^2Q_1^2\right)+\frac{1}{2}\left(\frac{P_2^2}{\mu_2}+\mu_2\omega_2^2Q_2^2\right)\pm\sqrt{V_1^2Q_1^2+V_2^2Q_2^2}$$

The condition of $V_2 \ll V_1$ is approximated by setting V_2 equal to zero, which gives:

$$H=\frac{1}{2}\left(\frac{P_1^2}{\mu_1}+\mu_1\omega_1^2Q_1^2\right)+\frac{1}{2}\left(\frac{P_2^2}{\mu_2}+\mu_2\omega_2^2Q_2^2\right)\pm V_1Q_1 \qquad (2)$$

Because the third term in eq 2 involves only one coordinate, it can be brought into the first term by completing the square.

$$H=\frac{1}{2}\left(\frac{P_1^2}{\mu_1}+\mu_1\omega_1^2\left(Q_1\pm\frac{V_1}{\mu_1\omega_1^2}\right)^2-\frac{V_1^2}{\mu_1\omega_1^2}\right)+\frac{1}{2}\left(\frac{P_2^2}{\mu_2}+\mu_2\omega_2^2Q_2^2\right) \qquad (3)$$

In this form, the Hamiltonian can be recognized as a sum of two separate Hamiltonians: one for motion along Q_1 and one for motion along Q_2. The Hamiltonian for motion along Q_2 is that for an unperturbed harmonic oscillator of frequency ω_2. For motion along the Q_1 coordinate, there is now a constant term in the potential, $-V_1^2/\mu_1\omega_1^2$, that simply shifts all the vibronic levels down in energy by the same increment. In addition, the coordinate is now $Q_1 \pm (V_1/\mu_1\omega_1^2)$ instead of Q_1. Nevertheless, inspection of the form of the Hamiltonian in eq 3 finds that the frequency of the mode is still ω_1, *unchanged from that of the mode in the absence of any Jahn–Teller interaction.* The entire effect of the Jahn–Teller distortion, in the case of $V_2 \ll V_1$, is to shift the vibronic levels down by $-V_1^2/\mu_1\omega_1^2$ and displace the equilibrium geometry along Q_1 by $\pm V_1/\mu_1\omega_1^2$, without changing the frequency of the vibration. The effective potential is schematically shown in Figure 4. Note that each vibronic energy level remains doubly degenerate, in contrast to the usual situation for a double-well potential; i.e., there is no tunneling splitting of degenerate vibronic levels in the $V_2 \ll V_1$ limit. Hougen[21] called this result an "accidental Born–Oppenheimer" case.

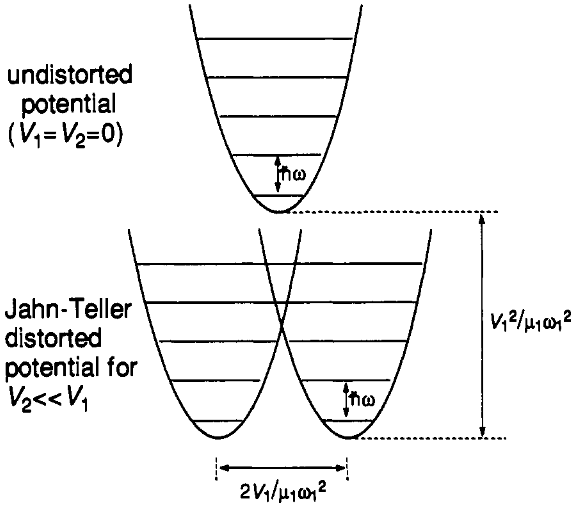

Figure 4. Schematic one-dimensional cut along Q_1 through a two-dimensional potential surface for the case $V_2 \ll V_1$. Vibronic energy levels are shown for the "accidental Born–Oppenheimer" potential surface. The upper curve shows the undistorted potential, e.g. $V_1 = V_2 = 0$.

For $\mathbf{1}^{\cdot+}$, our own ab initio calculations (see below) find a minimum at a rectangular geometry, 9.5 kcal/mol below the optimum square structure. The best rhomboidal structure lies on a saddle point 1.4 kcal/mol below the square. The geometries and energies compare well with the earlier work by Borden. With the Jahn–Teller stabilization energy along the b_{1g} coordinate much larger than that along the b_{2g} coordinate, we suggest that an accidental Born–Oppenheimer potential surface is a good approximate description for $\mathbf{1}^{\cdot+}$. Compared to the vibrational wave functions for the undistorted case, $V_1 = V_2 = 0$, those for $V_2 \ll V_1$ are approximately the same harmonic oscillator wave functions, displaced along Q_1 and shifted down uniformly in energy. The Franck–Condon factors are just those of a displaced harmonic oscillator, justifying the assumption that even Jahn–Teller-distorted $\mathbf{1}^{\cdot+}$ can be modeled using a harmonic potential.

Simulation of the Photoelectron Spectrum of 1. As a starting point for the simulations, we optimized the geometries and harmonic frequencies of **1** and $\mathbf{1}^{\cdot+}$ at the 6-31G+*/MP2 level.[24,25] Both optimized to rectangular D_{2h} structures at this level. The geometries and energies, listed in Table I, are in good agreement with earlier studies. The ionization potential taken from the ab initio energies, 7.53 eV, is lower than our experimental value of 8.16 ± 0.03 eV, presumably due to differences in the amount of correlation energy recovered in the calculations for the neutral versus the cation. The difference is not particularly unusual for a system of this size. We use the harmonic force field at the local

---

(24) Calculations were performed on an IBM RS6000 workstation using Gaussian 90: M. J. Frisch, M. Head-Gordon, G. W. Trucks, J. B. Foresman, H. B. Schlegel, K. Raghavachari, M. A. Robb, J. S. Binkley, C. Gonzalez, D. J. DeFrees, D. J. Fox, R. A. Whiteside, R. Seeger, C. F. Melius, J. Baker, R. L. Martin, L. R. Kahn, J. J. P. Stewart, S. Topiol, and J. A. Pople, Gaussian Inc., Pittsburgh, PA, 1990.

(25) For the open-shell cations, UMP2 wave functions gave satisfactory values of S^2 within 0.005 of the expected 0.7500.

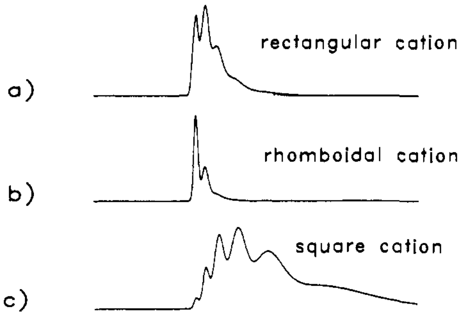

Figure 5. Comparison of simulated photoelectron spectra for rectangular **1** going to optimum (a) rectangular $\mathbf{1}^{\bullet+}$, (b) rhomboidal $\mathbf{1}^{\bullet+}$, and (c) square $\mathbf{1}^{\bullet+}$.

minima to calculate Franck–Condon factors for photoionization. The vibrational overlap integrals were computed in a mass-weighted Cartesian representation[11] which gives valid results even for cases of large change in equilibrium geometry. In particular, it properly handles the Duschinsky rotation that accompanies geometry change. The results, before and after convolution with an instrument function, are shown in Figure 2. A good simulation of the observed photoelectron spectrum is obtained with a very small adjustment of the ab initio geometry of $\mathbf{1}^{\bullet+}$. Adjusting only the C–C bond lengths[26] by 0.012 Å from the ab initio prediction gives a surprisingly good match to the experimental spectrum. This increment is a factor of 2 less than the 0.025-Å error bounds that we had found in a similar fitting[10] of the structure of c-$C_3H_2^{\bullet+}$. Simulations for ionization of rectangular **1** to give rhomboidal and square $\mathbf{1}^{\bullet+}$ (geometries optimized with rhomboidal or square constraints) are shown in Figure 5. Unreasonably large adjustments to the geometries would be needed to bring the simulations into conformity with experiment if the structure of $\mathbf{1}^{\bullet+}$ were in fact rhomboidal or square.

Conclusion

We have obtained a photoelectron spectrum of cyclobutadiene with partial vibrational resolution, from which we can measure the IP and deduce the Jahn–Teller-distorted radical cation of cyclobutadiene is rectangular at its equilibrium geometry. This confirms the predictions by ab initio calculations, in which correlations of both σ and π electrons were needed to predict the correct geometry.

Acknowledgment. Support from the Petroleum Research Fund, administered by the American Chemical Society (Grant 19726-G4), the Department of Energy (Grant DE-FG02-90ER14132), and the National Science Foundation (Grant CHE-9123487) is acknowledged.

---

[26] Adjustments to the geometry were done by recalculating the normal modes, and vibrational wave functions, of $\mathbf{1}^{\bullet+}$ at the adjusted geometry using the force constants (in internal coordinates) extracted from the ab initio geometry. The procedure, justified in ref 10, works for small (up to 0.025 Å) adjustments because the Franck–Condon factors depend strongly on geometry changes but only weakly on the numerical values of the force constants. The envelope resolution does not allow distinguishing between a very small C–C bond length change and a small CCH bond angle change.